Relative pinning strength of twin boundaries and outgrowths in $YBa_2Cu_3O_7$ thin films and superlattices

S. Berger,* D-G. Crété, J-P. Contour, K. Bouzehouane, and J-L. Maurice
Unité Mixte de Physique CNRS/Thomson-CSF, Domaine de Corbeville, 91404 Orsay, France

O. Durand
Laboratoire Central de Recherche de Thomson-CSF, Domaine de Corbeville, 91404 Orsay, France
(Received 21 July 2000; revised manuscript received 18 October 2000; published 19 March 2001)

$YBa_2Cu_3O_7$ films and superlattices displaying various structural properties were synthesized. X-ray diffraction, scanning electron microscopy, and transmission electron microscopy characterization reveal that the defect densities can be changed over a large range of magnitude. In particular, by controlling the strain relaxation in the material, superlattices without twin boundaries as well as highly twinned ones are deposited. ac susceptibility measurements are performed on many samples. Using a recent procedure based on flux-creep models, the relaxation rate of the vortices as a function of temperature is plotted in the region of large creep. The qualitative correlation between the defects densities (outgrowths, twins) and the pinning properties provides a description of the pinning landscape. Twin boundaries seem to play a preponderant role in vortex pinning. Intersections between the twin planes are believed to be the main pinning sites when present in our samples.

DOI: 10.1103/PhysRevB.63.144506 PACS number(s): 74.60.Ge, 74.62.Dh, 74.80.Dm, 74.76.Bz

I. INTRODUCTION

Vortex pinning has been studied in many works over the last several years. This is of great interest for understanding superconducting material properties, and a central issue for applications. Concerning copper oxide superconducting thin films, some applications in electronics (flux-flow transistors,[1] and Giaever transformers[2]) are based on vortices in motion that then require a great vortex mobility. Therefore, a very low pinning energy U is required.

These parameters determine the magnetic properties of the sample and can be investigated by measuring the ac susceptibility χ and deriving the vortex relaxation rate $S = k_BT/U$. Plotting $S(T)$ from low temperature to T_C is reliable to explore different successive behaviors for the vortex population. A study at relatively low temperature[3] describes the vortex phase diagram and displays the temperature limits, for different ac fields, of the vortex lattice. Hypotheses on the domain boundaries of the collective flux creep are formulated. The validity of the hypotheses on the collective flux creep is discussed. In the present work, we focus on the higher-temperature region, where the pinning effects are reduced. This domain is defined by the irreversibility temperature T_{irr}, above which depinning is thermally activated, and thermally activated flux flow (TAFF) is observed.[4] In this region, the zero voltage state vanishes, and the flux-creep equations are not relevant anymore. The $S(T)$ law should display a sharp change for $T = T_{irr}$, but in fact the threshold is not so clear. T_{irr} is sometimes defined as the peak temperature T_{peak} of the $\chi''(T)$ curve. This criterion cannot be invoked here, because T_{peak} is frequency dependent,[5] and our $S(T)$ curves are built out from measurements made at different frequencies and single temperatures. These issues have already been discussed by Tinkham,[6] and a criterion may be helpful to define the limits of the reversibility region. Thermal fluctuations are already efficient even for $k_BT < U$ and one can define a boundary of the TAFF region by $U < 20k_BT$, i.e., $S > 0.05$. This criterion is justified by the fact that the depinning, defined as an activation process, can be determined from the equation[7]

$$U = k_B T_{irr} \ln \frac{t}{t_0}, \tag{1}$$

with t the time scale of the experiment (in the range 10^{-3}–$10^{-5}s$) and t_0 the characteristic time scale of the vortex depinning ($t_0 \sim 10^{-11}s$). At the irreversibility line, one should obtain U/k_BT_{irr} between 15 and 20, in good agreement with our value. This criterion proves to be very efficient for establishing a difference between samples displaying various pinning properties. The higher the pinning energy, the narrower the TAFF temperature domain below T_C.[8]

$YBa_2Cu_3O_7$ (YBCO) thin films are known to have high critical current densities[9,10] and pinning energies.[11,12] Different kind of defects are present in copper oxide films. Each of them is able to play a role in the pinning mechanism, as soon as it constitutes a potential well for vortices, with at least one transversal dimension on the order of magnitude of the coherence length. Many works investigate the origin of pinning in high-temperature superconductor materials, and particularly in films. No clear feature is established up to now. Recently, the correlation between the dislocation density and the critical current density in YBCO films has been studied,[13] and the authors claimed that dislocations normal to the films were the main pinning sites in these materials. This assumption provides helpful information in this field. Nevertheless, one must be cautious before concluding. First, this is because films present various morphological properties, depending on the growth method and the deposition parameters. Second, in a given sample, many different defects families are found,

and a very exhaustive description of the ''landscape'' is the only means of having a precise idea of the vortex behavior. Moreover, some structural properties are often correlated to each other (dislocations with growth islands, roughness with film thickness, outgrowth morphology with crystalline quality), and interpretations become very tricky. In any case, any evidence for the influence of a defect on the film pinning properties is a positive step, if we do not conclude too quickly, and if it helps to improve the material for application.

To this aim, we studied the influence on pinning of two kinds of defects in our films. On the one hand, we have measured several YBCO films that present various outgrowth densities, depending on the deposition parameters used. Outgrowths are large volume defects (diameters between 50 nm and 1 μm) including various phases. Always present in films synthesized by the laser ablation method, we believe that they are able to pin the vortices at the interface with the superconducting volume, or even inside the defect. On the other hand, we have measured four superlattices $YBa_2Cu_3O_7/PrBa_2(Cu_{1-x}Ga_x)_3O_7$ (YBCO/PBCGO), displaying various twinning, in order to study the influence of twin boundaries (TB's) on the pinning properties. Indeed, in previous studies, we have shown that the YBCO/PBCGO superlattices may be tetragonally strained on the $SrTiO_3$ (STO) cubic lattice if the thickness of the YBCO elementary layer is low enough (<4 uc), but it also depends on the substrate miscut orientation with respect to the in-plane axes and on the miscut angle with respect to the (100) surface.[14] When the superlattice is tetragonally strained, no evidence of the twinning along the $[110]$ and $[1\bar{1}0]$ directions—typical of the YBCO thick films deposited on STO—is found in transmission electron microscopy (TEM) plane views, as in ultrathin YBCO films.[15,16]

II. PINNING ENERGY

Pinning centers attract vortices with a force depending on their distance; the work of the force required to extract a pinned vortex out of the interaction range is equal to the pinning potential U. A current flowing in a thin film generates a Lorentz force acting on the vortices. As this force helps an individual vortex to escape from the pinning center by thermal activation (strong individual pinning), the effective pinning energy U is lowered by the current density J. This dependence has been first modeled by Anderson and Kim[43] in their description of the flux-creep regime by the simple analytical form

$$U(J)=U(0)\left(1-\frac{J}{J_c}\right), \tag{2}$$

where J_c is the critical current density separating the flux-creep from the flux flow regimes. The latter is characterized by an ohmic behavior and appears for $J>J_c$. A model developed by Bardeen and Stephen[17] gives the flux-flow resistivity of type II superconductors, $\rho_{FF}=\rho_N\cdot(B/B_{C2})$ where ρ_N is the normal-state resistivity.

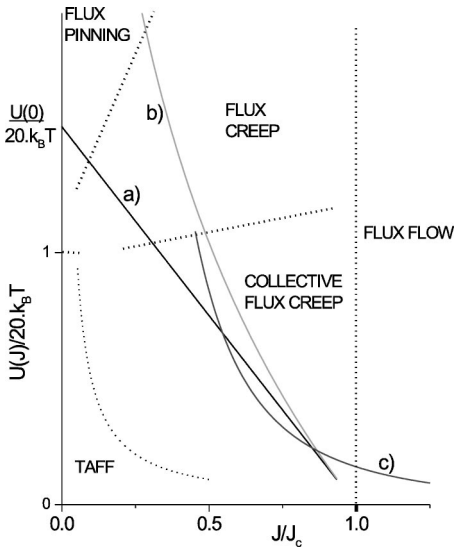

FIG. 1. Representation of the different regimes of vortex dynamics on a $(J/J_c, U/20k_BT)$ diagram; the dotted lines separate the corresponding domains, and the plain lines describe the behavior of a sample according to the models of (a) Anderson-Kim (Ref. 43), (b) Zeldov (Ref. 19), and (c) collective flux creep. At low temperature as assumed on the graph, $U(0,T)>20k_BT$, so that the TAFF regime is not observed. This regime is separated from the flux-pinning regime by the condition $U=20k_BT$ for $J\sim 0$. At higher current densities, the limit of the TAFF regime is given by (J/J_c). $(U/k_BT)\ll 1$.

A third regime is observed when U is not large compared to k_BT: the vortices are not pinned and move in a reversible regime at low current densities (TAFF). TAFF is observed experimentally as a nonzero resistance for $J\ll J_c$. We can use the criterion $U(0)<20k_BT$ to draw the diagram of Fig. 1, describing the different regimes in reduced coordinates $(J/J_c, U/20k_BT)$. On this figure appear two other proposed dependencies of $U(J)$.

(1) The following relationship is proposed using a model of collective flux creep (i.e., for $J\sim J_c$):

$$U(J)=U(J_c)\cdot\left(\frac{J_c}{J}\right)^{\mu}, \tag{3}$$

where μ depends on the size of the vortex bundle[18] and usually varies from $\frac{1}{7}$ to $\frac{5}{2}$.

(2) The model proposed by Zeldov *et al.*,[19] accounting for a logarithmic barrier deduced from experiments on magnetic relaxation rates,

$$U(J,T,H)=U(T,H)\cdot\ln\left(\frac{J_c}{J}\right), \tag{4}$$

where H is the applied magnetic field. This empirical result yields, together with the Arrhenius law for the electric field,

$$E(J)=E_0\exp\frac{-U(J)}{k_BT}, \tag{5}$$

a power law for the V-I curve, often verified by transport measurements[20,21]

$$E(J)=E_0\left(\frac{J}{J_C}\right)^n, \tag{6}$$

where

$$n=\frac{U}{k_BT} \tag{7}$$

is the so-called flux-creep exponent.

In order to compare the pinning energy for various samples, we follow an extraction algorithm recently proposed by Jönsson *et al.*[22] The authors extract the flux-creep exponent, well defined in the flux-creep regime, or the relaxation rate

$$S=\frac{1}{n} \tag{8}$$

as a function of temperature, from a single temperature scan of ac-magnetic-susceptibility measurements at several frequencies. Within the frame of the critical state model, we can approximate the ac susceptibility of a thin circular disk by the simple form[23]

$$\chi' \sim -\frac{8R}{3\pi d}c_1 h^{-3/2}, \tag{9a}$$

$$\chi'' \sim -\frac{8R}{3\pi d}c_2 h^{-1} \tag{9b}$$

in the limit $h \gg 1$, where $h=2H_0/J_c d$ is the reduced field, H_0 is the amplitude of the ac field, R is the radius of the film, d is its thickness, and c_1 and c_2 are numerical factors. Therefore,

$$\chi' \propto J_c(T,H_0,f)^{3/2}. \tag{10}$$

Using results of the collective flux-creep theory[24] in the framework of the critical state formalism,[25] the frequency dependence of the critical current density can be described by the power law

$$J_c(T,H_0,f)=J_c(T,H_0)\left(\frac{f}{f_0}\right)^{1/n}. \tag{11}$$

By combining this relation with the flux-creep Eq. (10), we obtain

$$\chi'(T,H_0,f)=K(T,H_0)f^{[3S(T,H_0)/2]}. \tag{12}$$

Thus, we are able to extract the so-called relaxation rate $S(T,H_0)$ from ac susceptibility measurements at various frequencies. In particular for a given H_0, a simple temperature scan directly provides the curve $S(T)$, which is much faster than the usual method for getting the critical current density from $T_{peak}(H_0)$ measurements. The comparison between the $S(T)$ curves and the irreversibility temperatures measured from two films provides a direct comparison between the two pinning energies. This method is a practical tool for the characterization of film pinning properties.

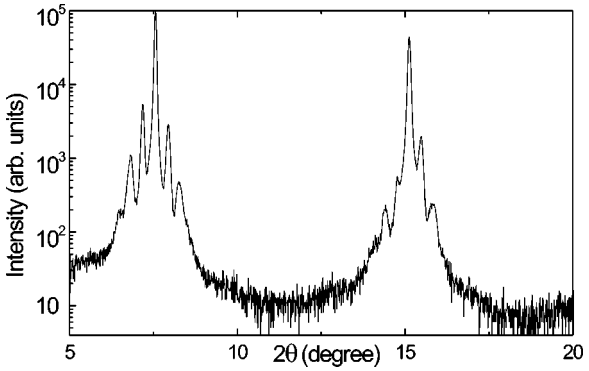

FIG. 2. 001 and 002 reflections of the $\theta-2\theta$ XRD pattern of a *c*-axis-oriented YBCO/PBCGO superlattice grown on STO (100) recorded using Cu (Kα) radiation (15YBCO uc/6PBCGO uc/10 periods; growth temperature $=785\,^{\circ}$C), yielding $\Lambda_{XRD}=25.3$ nm.

III. EXPERIMENT

Films and superlattices were prepared *in situ* by pulsed laser deposition in a multitarget LDM 32 Riber machine using a frequency-tripled Nd:yttrium aluminum garnet laser (B.M. Industries 503 DNS) with a pulse length of 5 ns at a repetition rate from 1–5 Hz. It delivers a laser beam at a 355-nm wavelength with a power density from 50–600 MW/cm^2 depending on the focus on the target. In this work, the growth parameters have been set in order to obtain a deposition rate at 0.3 nm/s for PBCGO and at 0.26 nm/s for YBCO at a repetition rate of 2.5 Hz and a substrate-target distance of 35 mm. The YBCO and PBCGO ($x=0.2$) targets were stoichiometric with a density exceeding 90% of the theoretical one. The PBCGO target was prepared at the Crown Center for Superconductivity at Technion University.[26] They are continuously moved to ensure a uniform ablation rate. Before the growth, the (100) STO substrates are cleaned by heating in pure oxygen up to 800 °C for 10 min at a pressure of 40 Pa. After this procedure, cleanliness and flatness of the surface are verified by reflection high-energy electron diffraction before starting the growth procedure. The growth temperature was 785 °C, measured at the surface of the substrate holder. The growth was carried out in 40 Pa of pure oxygen, while the substrate holder was continuously rotated at 45 rpm. At the end of the deposition, the pressure was increased to 4 10^4 Pa. The sample was then cooled to room temperature within 45 min including an intermediate temperature plateau at 400 °C during 15 min.

X-ray-diffraction (XRD) analysis has been carried out by using $\theta-2\theta$ and four-circle x-ray diffractometers in Bragg-Brentano geometry with Cu(Kα) sources. The growth rates are calibrated from $\theta-2\theta$ XRD measurements performed on a set of two calibration superlattices and from low angle x-ray reflectometry on thin (<50 nm) YBCO and PBCGO layers deposited on STO. The period of the studied superlattices is then controlled by XRD after the growth,[27] as shown in Fig. 2, which presents a typical $\theta-2\theta$ diffraction pattern recorded from a $(15\text{YBCO}/6\text{PBCGO})_{10}$ superlattice. All superlattices contain 10 periods, the growth being initiated by the PBCGO layer. It is then encapsulated by a PBCGO layer

TABLE I. Thickness (t), roughness average (Ra), and outgrowth density (*Doutg*) of the YBCO films.

Sample	t (nm)	Ra (nm)	*Doutg* (cm^{-2})
LDM443	100	2	510^5
AL962	50	3	2.110^7
AL971	300	6	4.410^7
AL1057	500	6	2.710^7

having the same thickness as the PBCGO layer of the elementary period.

The films are cooled in a flow cryostat Oxford CF1200. The temperature is measured near the sample by a Si diode, using steps of 0.1 K and a 0.03-K relative accuracy. A 10-mT dc field normal to the film is applied during the measurements to ensure that $H_{AC} \ll H_0$ and that external conditions are identical for all the measurements. The excitation magnetic field is applied normally to the film, with an amplitude of 0.5 mT at frequencies varying from 1 kHz–100 kHz. The magnetic susceptibility measurements are performed in the screening configuration. The $10 \times 10\,mm^2$ film is placed between two coils (diameter 5 mm).

In order to calibrate all our measurements, the signal is assumed to be totally screened by the superconducting material in the low-temperature state (i.e., $\chi'' = -1$ in this temperature range). This assumption is justified by the fact that the real part of the ac susceptibility measures the variation of the magnetization, depending on the flux-line mobility. In the low-temperature critical state, if present, they are totally pinned. In the normal state, we can neglect the eddy currents in these low-conductivity materials, so that $\chi'' = 0$.

Flux creep only appears at higher temperature. We plot χ' as a function of the signal frequency for different temperatures. As explained above, we directly obtain the $S(T)$ curve.

IV. RESULTS

A. YBCO films

For more clarity, we display results concerning four YBCO films that are representative by their deposition parameters, structure, and outgrowth densities of many other films measured in the same way. Morphological characteristics of these films are summarized in Table I. These parameters are of great importance for the interpretation of the pinning mechanisms, since the correlation with the magnetic measurements quantifies the pinning properties of the defects.

The density of dislocations is not known, and the twinning due to the relaxation mechanism is supposed to be roughly constant, and much larger than the flux-line density during the measurements (see Fig. 3).

Figure 4 displays normalized $\chi'(T)$ and $\chi''(T)$ curves at several frequencies for sample AL962. Defining T_C^{onset} as the minimum temperature where $\chi' = 0$, we determine T_C as the extrapolation of the T_C^{onset} at infinite frequency.

As a general feature, the high-temperature part of the $\chi(T)$ curves and critical temperatures for $H_0 = 10$ mT are

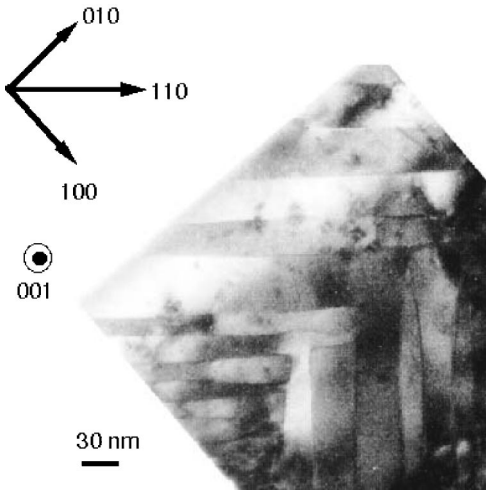

FIG. 3. TEM picture of TB's in a YBCO film.

actually not shifted as compared to the $H_0 = 0$ measurement. The frequency dependence is very similar. This behavior, usual at a temperature close to the transition, is characteristic of the flux-flow regime.

A finite response is obtained only in a very narrow temperature range below T_C. This means that very strong vortex pinning is provided by deep potential wells. Thermal depinning and flux creep occur very close to T_C, where fluctuations appear and penetration length diverges. In this case, vortex depinning by a pure activation process is unlikely, since the vortex structure goes through transformation. If the critical temperature were increased, flux creep would occur at higher temperature in the same way.

$S(T)$ for the film AL962 is plotted in Fig. 5. The criterion $S = 0.05$ chosen for determining the irreversibility leads to $T_{irr} = 85.9$ K. Similar remarks could be made for the other samples.

Figure 6 displays the $S(T)$ curves of the four films around the criterion value, where we use the reduced temperature $T = T/T_C$ to make the curves directly comparable [because in this case, $U(T)$ varies much more than $k_B T$]. A noticeable difference exists between the four reduced irreversibility temperatures, i.e., between the pinning energies averaged

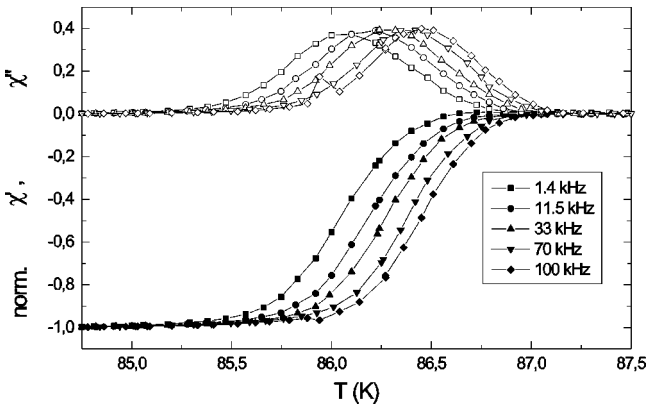

FIG. 4. Real and imaginary parts of the ac-magnetic susceptibility as a function of temperature for different frequencies.

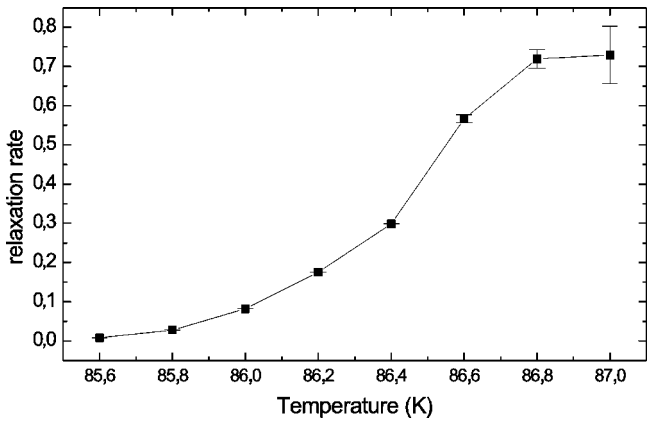

FIG. 5. $S(T)$ curve of the YBCO film AL962.

over the whole samples. Indeed, this relative variation in the temperature, where fluctuation-induced depinning occurs, provides information on how large U is compared with k_BT. The larger U/k_BT is, the stronger the fluctuations must be to induce depinning, and the higher the T_{irr}. As a consequence, the sample AL971 displays the highest pinning energy in this temperature range, and LDM443 the lowest. More than 10 films were measured in this way. We noticed that the thickness has no systematic effect on the results, nor does the surface roughness. Only the outgrowth density seems to be slightly correlated with T_{irr}. This trend is shown in Fig. 7. The plot dispersion can be explained by the irregular outgrowth density over each film.

The error bars relative to $S(T)$ measurements (coming from the normalization of the susceptibility curves and the fitting procedure) do not discard this trend. These results show that the outgrowths have an incidence on the vortex pinning. Several theoretical works describe pinning by nonsuperconducting inclusions[28,29] in the volume of the defects or at the boundary. Peculiarly, experimental results are lacking.

The outgrowth concentration, if close to the vortex density, is very sensitive too. We are not able to provide a precise description of this mechanism and we do not assert that these kinds of defects are the main pinning sites in our films.

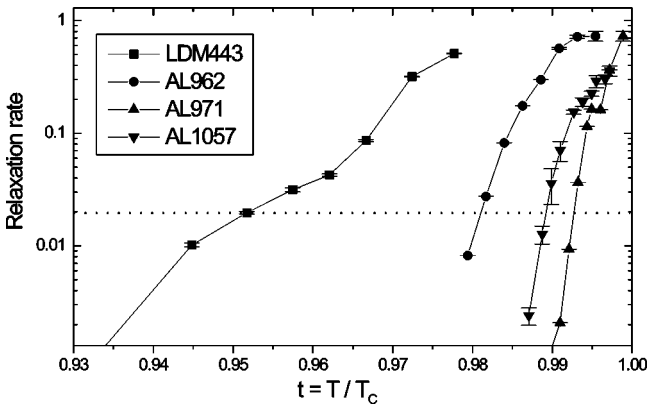

FIG. 6. $S(T)$ curves of the single YBCO films. The dotted line corresponds to the irreversibility criterion.

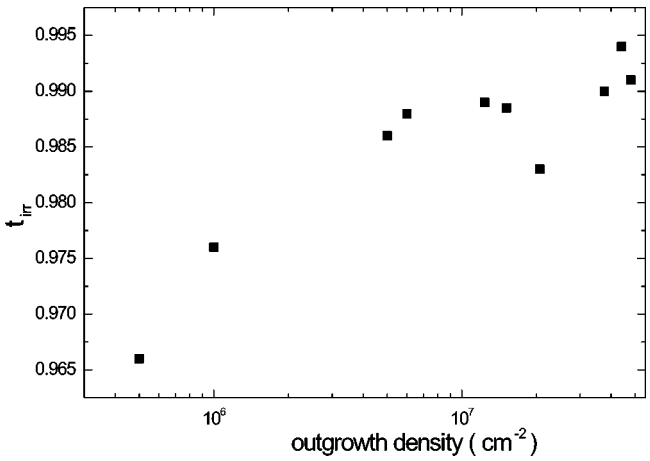

FIG. 7. Reduced irreversibility temperature of the single YBCO films as a function of their outgrowth density.

Nevertheless, we believe that such large and numerous defects influence vortex dynamics and pinning.

B. Superlattices

The superlattices showing the shortest periods (AL1319 and AL1235) are strongly tetragonally strained as shown by the XRD data reported in Table II. Although AL1235 was not analyzed using four-circle XRD, we observed a *c*-axis lattice parameter consistent with a strained $YBa_2Cu_3O_7$ film and the full width at half-maximum (FWHM) of the rocking curve of the (005) YBCO reflection is very narrow and characteristic of an epitaxial growth.[14,30] Stress relaxation barely appeared in sample AL1318, as seen from $\theta-2\theta$ diffraction on (308). There is no evidence of twinning as measured by a Φ scan on the (227) planes (Φ is the angle of rotation around the direction normal to the surface of the sample). The sample with the thicker YBCO layers, AL1481, is a relaxed structure showing properties close to those of single YBCO thick films, such as (i) FWHM of the rocking curves of the (005) reflection, (ii) Φ scan on the (102), (227), and (038/308) reflections, and (iii) a twinning rate.

In such relaxed films and heterostructures, the twinning takes place about the (110) and $(1\bar{1}0)$ planes of YBCO; therefore, in absence of symmetry breaking (for example the miscut orientation and angle), both domains should have the same weight.[15,31] All of these samples display comparable outgrowth densities ($\sim 10^7\ \mathrm{cm}^{-2}$).

Figure 8 displays the $S(T)$ curves for the four superlattices. The critical temperature is given for each sample. It is dramatically reduced for the superlattices with the thinner YBCO layers, in good agreement with previous studies.[32,33] For this reason, the choice of a temperature scale is tricky. The use of the linear scale is justified below; the temperature ranges where pinning is inefficient are much larger for three superlattices (AL1319, AL1235, and AL1318) than for the fourth (AL1481), which behaves like single YBCO films. Concerning AL1319, AL1235, and AL1318, the irreversibility temperature is far from T_C (between 10–15 K below), which indicates that the vortex depinning that happens during the measurement is fundamentally different from the

TABLE II. Summary of the XRD analysis of a YBCO thin film and the superlattices $[(YBCO)_M/(PBCGO)_N]_{10}//STO$.

Sample	Λ (nm) M,N	Parameter (Å)	FWHM (005) (degrees)	FWHM (102) (degrees)	FWHM (227) (degrees)	Twinning rate $\langle 110 \rangle$ (227)	FWHM (038/308) (degrees)
AL1319	11.47	$a=3.895$					
	$M=3,N=6$	$b=3.895$	0.108	0.41	0.53	N.D.	0.50
		$c=11.749$					
AL1235	11.0	$a=$ } not measured					
	$M=4,N=5$	$b=$ }	0.190				
		$c=11.7135$					
AL1318	31.0	$a=3.860$					
	$M=9,N=18$	$b=3.910$	0.470	0.57	0.77	N.D.	0.78
		$c=11.740$					
AL1481	25.3	$a=3.842$					
	$M=15,N=6$	$b=3.896$	0.315	0.78	0.67	0.56/0.44	0.65
		$c=11.714$					
AL959	100	$a=3.825$					
(film)		$b=3.889$	0.384	0.77	0.57	0.51/0.49	0.62
		$c=11.687$					

mechanism invoked with the single films. Indeed, the thermal energy k_BT is compared with the pinning energy $U(T)$. k_BT increases linearly with the temperature, whereas $U(T)$, quantifying the interaction between a vortex and a pinning site, decreases very slowly at low temperature and vanishes close to T_C because of the divergence of the size of the vortex. Then, for T_{irr} close to T_C, in which case, as explained above, other mechanisms are involved, we can compare two samples by assuming that there is an unique activation process quantified by the well-defined pinning energy. The use of the reduced temperature scale is then fully justified. However, for the superlattices, the thermal depinning energies must be underscored. Therefore, we prefer the linear temperature scale in this case (anyway, a reduced scale would not qualitatively change the trend). Analyzed in this way, the $S(T)$ curve reveals that the four superlattices have pinning energies that are strongly different at a given temperature (in increasing energies: AL1319, AL1235, AL1318, and AL1481). The use of the reduced temperature as we have used for the single films, would provide, we believe, an incorrect picture, because of the large critical temperature differences. Nevertheless, we can notice that T_{irr}/T_C is dramatically reduced for the strained superlattices, as compared to the relaxed one (AL1481).

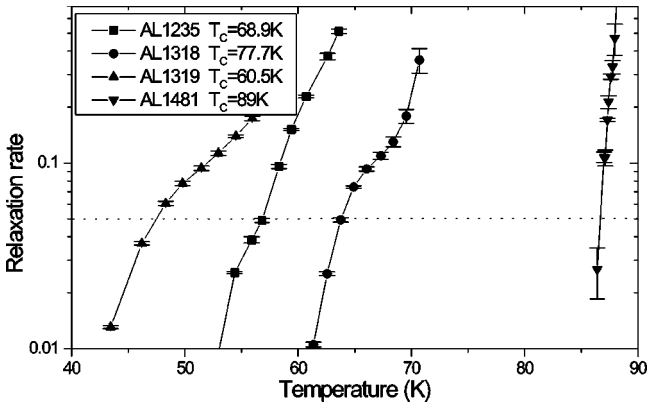

FIG. 8. $S(T)$ curves of the superlattices. The dotted line corresponds to the irreversibility criterion.

The pinning properties of the superlattice AL1481 are identical to those of YBCO films. The twinning is very similar in the two cases and strong pinning by TB's seems to be an accurate hypothesis. Concerning the three other superlattices, the pinning energy given above decreases with increasing strain measured by x-ray diffraction, and following, with decreasing twin boundaries concentration.

V. DISCUSSION

Outgrowths and twin boundaries are found to influence the pinning properties, and no correlation with other defects was established. In bulk materials, many experimental evidences prove the role of TB's in pinning properties.[34–37] If the vortex motion is normal to the TB planes, they constitute strong pinning centers, whereas if the vortices move in the same direction as the TB planes, they act as grooves channeling the flux lines.[38] In the present case, TB's are present in two directions with an angle of 90°, at $\pm 45°$ with respect to the sides of the substrate and to the vortex motion directions. Anyway, the channeling mechanism should happen if the transverse pinning force induced by the twin boundary on a flux line is strong enough to keep it in the potential groove. Then, the vortex will move along it until it reaches a twin boundary intersection. The interboundary spacing is less than 100 nm in these films. The vortex can then be pinned or again channeled in a direction normal to the previous one. The intersection between two TB's induces a local perturbation in the crystallographic order that constitutes effective

pinning sites.[39] These defects are present with a high concentration in the relaxed films and disappear abruptly in the strained samples. We assume that these defects are potential wells deeper than a twin boundary for a free isolated vortex.

Ravelosona *et al.*[40] have studied the irreversibility line by magnetization measurements in strained superlattices very similar to ours (1–4YBCO/4PBCGO). They find irreversibility temperatures in good agreement with our measurements. They assume that the vortex arrays are decoupled, but can adopt a three-dimensional behavior in each superconducting layer. Then, the superlattices should be considered as equivalent to a collection of thin independent YBCO films. As a consequence, the decreasing thickness of the YBCO layers induces a reduction of the condensation energy, and then, of the pinning energy at zero temperature. Unfortunately, this effect works in the same direction as the reduction of the TB concentration. Therefore, no definitive conclusion can be proposed concerning the role of these defects. Nevertheless, the qualitatively different behavior of the strained superlattices tends to show that another pinning mechanism is involved. Therefore, we do believe that TB's are effective pinning centers in our films.

The role of the outgrowths is not clear. In relaxed films, these defects seem to slightly favor pinning. In strained superlattices, such a behavior could not be established. A pinning mechanism including several defects (TB's and outgrowths) could be invoked. Nevertheless, the pinning energies have not been measured and a systematic comparative study including several pinning defects is lacking. Additional measurements are then required.

Two recent works[41,42] study the role of TB's by measuring YBCO films twinned in one direction only. They both find highly anisotropic critical current densities and resistivity, and conclude that TB's have an effective channeling effect. In this case, where no intersection of TB's is present, TB plans seem to be governing the vortex dynamics. Villard *et al.*[41] have measured the critical current density with the current parallel and perpendicular to the TB's, and have found $1.2\,10^6 A\,\mathrm{cm}^{-2}$ and 25 times less, respectively, at 77 K. This anisotropy is a clear demonstration of the role of twins in pinning mechanisms. Moreover, at this temperature, our films display critical current densities close to $10^7 A\,\mathrm{cm}^{-2}$. These higher values suggest that pinning by defect intersections is predominant. The discrimination of the effect of one particular defect requires a precise control of the microstructure. Films with an unique twinning direction have been synthesized. Further measurements are being processed on such samples in order to test the above hypothesis, and will be reported elsewhere. Preliminary results show that these samples have a T_C as high as the present YBCO films, but a much lower temperature of irreversibility. Moreover, these films display anisotropic transport properties. These facts corroborate the above analysis.

VI. CONCLUSION

We have synthesized YBCO films with various densities of defects capable of pinning the vortices. X-ray-diffraction measurements and TEM imaging reveal the twin boundary density due to the strain relaxation in the films. A simple processing of ac-magnetic-susceptibility data enables us to compare the pinning energies, and to correlate them to the defect densities. This qualitative study provides information on the effective pinning sites in our films. On the one hand, outgrowths are believed to have a real effect on pinning properties in single YBCO films with high TB densities, even if no precise mechanism is proposed. On the other hand, the disappearance of TB's in superlattices induces a drop in the zero-temperature pinning energy. Pinning by the twin planes and by the intersection between two perpendicular TB's is invoked. This last kind of defect is believed to be the effective pinning site in our YBCO films. Further experiments are proposed in order to establish if TB's are the dominant defects in the pinning landscape of these materials.

ACKNOWLEDGMENTS

The authors thank B. J. Jönsson for extensive discussions on results, E. Jacquet for his helpful contribution in film and superlattice elaboration, and C. Dolin for performing XRD analyses. They are also grateful to B. Fisher and L. Patlagan (Technion, Haifa, Israel) for supplying the PBCGO targets used in this study.

*Present address: CEA-Saclay, SPEC Orme des Merisiers, 91191 Gif-sur-Yvette Cedex, France. Email address: sberger@drecam.saclay.cea.fr

[1] P. Bernstein, C. Picard, V. Becker, S. Flament, and N. Beaudet, J. Appl. Phys. **78**, 7358 (1995).
[2] S. Berger, K. Bouzehouane, D. Crété, and J. P. Contour, Eur. Phys. J. A **6**, 111 (1999).
[3] B. J. Jönsson (private communication).
[4] P. H. Kes, J. Aarts, J. van der Berg, C. J. van der Beek, and J. A. Mydosh, Supercond. Sci. Technol. **1**, 242 (1989).
[5] S. Takács and F. Gömöry, Inst. Phys. Conf. Ser. **158**, 993 (1997).
[6] M. Tinkham, Phys. Rev. Lett. **61**, 1658 (1988).
[7] L. Burlachkov, V. B. Geshkenbein, A. E. Koshelev, A. I. Larkin, and V. M. Vinokur, Phys. Rev. B **50**, 16 770 (1994).
[8] T. T. M. Palstra, B. Batlogg, R. B. van Dover, L. F. Schneemeyer, and J. V. Waszczak, Phys. Rev. B **41**, 6621 (1990).
[9] M. Ye, J. Schroeder, M. Mehbod, R. Deltour, A. G. M. Jansen, and P. Wyder, Physica C **258**, 95 (1996).
[10] X. Xu, J. Fang, X. Cao, and K. Li, Solid State Commun. **93**, 291 (1995).
[11] P. Bernstein, C. Picard, M. Pannetier, Ph. Lecœur, J. F. Hamet, T. D. Doan, J. P. Contour, M. Drouet, and F. X. Régi, J. Appl. Phys. **82**, 5030 (1997).
[12] X. Xiaojun, F. Lan, W. Liangbin, Z. Yuheng, F. Jun, C. Xiaowen, L. Kebin, and S. Hisashi, Phys. Rev. B **59**, 608 (1999).
[13] B. Dam, J. M. Huijbregtse, F. C. Klaassen, R. C. F. van der Geest, G. Doornbos, J. H. Rector, A. M. Testa, S. Freisem, J. C. Martinez, B. Stuble-Pmpin, and R. Griessen, Nature (London) **399**, 439 (1999).
[14] J. P. Contour, A. Abert, and A. Défossez, Proc. SPIE **2697**, 339 (1996).
[15] J. L. Maurice, O. Durand, M. Drouet, and J. P. Contour, Thin

Solid Films **319**, 211 (1998).
[16] J. P. Contour, M. Drouet, O. Durand, J. L. Maurice, and A. Gauzzi, Physica C **282-287**, 689 (1997).
[17] J. Bardeen and M. J. Stephen, Phys. Rev. **140**, A1197 (1965).
[18] V. M. Vinokur, P. H. Kes, and A. E. Koch, Physica C **248**, 179 (1995).
[19] E. Zeldov, N. M. Amer, G. Koren, A. Gupta, M. W. McElfresh, and R. J. Gambino, Appl. Phys. Lett. **56**, 680 (1990).
[20] E. Zeldov, A. I. Larkin, V. B. Geshkenbein, M. Konczykowski, D. Majer, B. Khaykovich, V. M. Vinokur, and H. Shtrikman, Phys. Rev. Lett. **73**, 1428 (1994).
[21] Z. H. Wang, K. B. Li, J. Fang, J. L. Chen, and X. W. Cao, Z. Phys. B: Condens. Matter **104**, 445 (1997).
[22] B. J. Jönsson, K. V. Rao, S. H. Yun, and U. O. Karlsson, Phys. Rev. B **58**, 5862 (1998).
[23] J. R. Clem and A. Sanchez, Phys. Rev. B **50**, 9355 (1994).
[24] M. V. Feigel'man, V. B. Geshkenbein, A. I. Larkin, and M. V. Vinokur, Phys. Rev. Lett. **63**, 2303 (1989).
[25] L. Fàbrega, J. Fontcuberta, S. Piñol, C. J. van der Beek, and P. H. Kes, Phys. Rev. B **47**, 15 250 (1993); L. Fàbrega, J. Fontcuberta, L. Civale, and S. Piñol, *ibid.* **50**, 1199 (1994).
[26] D. Ravelosona, J. P. Contour, M. Drouet, B. Fisher, and L. Patlagan, J. Alloys Compd. **251**, 209 (1996).
[27] I. K. Schüller, Phys. Rev. Lett. **44**, 1597 (1980).
[28] S. Tokuono, S. Tanaka, and H. Fukuyama, Physica C **185-189**, 2283 (1991).
[29] H. R. Kerchner, Cryogenics **29**, 251 (1989).
[30] M. Ece, E. Garcia-Gonzals, and H. U. Habermeier, J. Appl. Phys. **77**, 1646 (1995).
[31] B. M. Lairson, S. K. Streiffer, and J. C. Bravman, Phys. Rev. B **42**, 10 067 (1990).
[32] J. M. Triscone, Ø. Fisher, O. Brunner, L. Antognazza, A. D. Kent, and M. G. Karkut, Phys. Rev. Lett. **64**, 804 (1990).
[33] R. G. Goodrich, P. W. Adams, D. H. Lowndes, and D. P. Norton, Phys. Rev. B **56**, R15 299 (1997).
[34] A. I. Larkin, M. C. Marchetti, and V. M. Vinokur, Phys. Rev. Lett. **75**, 2992 (1995).
[35] A. Umezawa, G. W. Crabtree, U. Welp, W. K. Kwok, K. G. Vandervoort, and J. Z. Liu, Phys. Rev. B **42**, 8744 (1990).
[36] S. Sanfilippo, A. Sulpice, O. Laborde, D. Bourgault, Th. Fournier, and R. Tournier, Phys. Rev. B **58**, 15 189 (1998).
[37] V. K. Vlasko-Vlasov, L. A. Dorosinskii, A. A. Polyanskii, V. I. Nikitenko, U. Welp, B. W. Veal, and G. W. Crabtree, Phys. Rev. Lett. **72**, 3246 (1994).
[38] V. M. Pan, in *Physics and Material Science of Vortex State, Flux Pinning and Dynamics, Advanced Studies Institute NATO* (Kluwer Academic Publishers, Dordrecht, The Netherlands, 1999), p. 1.
[39] M. Oussena, P. A. J. de Groot, S. J. Porter, R. Gagnon, and L. Taillefer, Phys. Rev. B **51**, 1389 (1995).
[40] D. Ravelosona, J. P. Contour, and N. Bontemps, Phys. Rev. B **61**, 7044 (2000).
[41] C. Villard, G. Koren, D. Cohen, E. Polturak, B. Thrane, and D. Chateignier, Phys. Rev. Lett. **77**, 3913 (1996).
[42] A. Casaca, G. Bonfait, C. Dubourdieu, F. Weiss, and J. P. Sénateur, Phys. Rev. B **59**, 1538 (1999).
[43] P. W. Anderson and Y. B. Kim, Rev. Mod. Phys. **36**, 39 (1964).